

Fault Diagnosis of a Propeller Using Sub-Nyquist Sampling and Compressed Sensing

YUKI KATO 

Department of Mercantile Marine, National Institute of Technology, Hiroshima College, Toyota-gun 725-0231, Japan

e-mail: kato.yuki.ws@alumni.tsukuba.ac.jp

ABSTRACT The fault diagnosis of rotating machinery is generally performed using methods that employ vibration and sound. These methods are simple and accurate. However, all of these methods measure vibration data on the basis of the sampling theorem. Thus, they require a high measurement frequency, resulting in a large data volume and expensive measurement equipment. In recent years, a method that uses compressed sensing has been proposed to solve this problem, but it requires dedicated hardware to realize random sampling. To overcome this drawback, we developed a random start uniform sampling method (RSUSM) and combined it with compressed sensing (CS). RSUSM is a method of measuring data at a fixed frequency with a random start time. Numerical experiments demonstrate how the specific constant changes for each RSUSM parameter. This allows us to know the limit of how many measurement points are required for the number of non-zero components. We also applied CS by RSUSM to the sound pressure measurement results of the failed propeller, and found that the signal could be recovered less than 25% error even in a noisy real environment within the aforementioned limit. In this case, we found that the measurement frequency could be compressed to 1/80th of the frequency required by the sampling theorem, and the measurement data size to 1%. This approach is expected to diagnose faults in more rotating machines by significantly reducing the costs associated with data collection and storage.


INDEX TERMS Compressed sensing, data compression, fault diagnosis, Fourier transforms, signal processing.

I. INTRODUCTION

Failures inevitably occur in rotating machinery owing to defects in materials, fatigue, and aging. Failures lead to equipment downtime, resulting in economic loss. Therefore, it is important to diagnose the failures of rotating machinery and maintain it in a working condition. Sound-based and vibration-based methods have been widely used to detect the failures of bearings [1], [2] gearboxes [3] propellers [4], [5] etc. because they are robust and failures can be detected at an early stage. Heng and Nor [1] compared the performance of various classical statistical parameters in bearing fault diagnosis using acoustic pressure and vibration signals. Hoang and Kang [2] showed that convolutional neural networks could diagnose bearing faults with high accuracy and robustness even in noisy environments. Randall *et al.* [3] conducted experimental and theoretical investigations to develop a method for diagnosing gearbox faults from the frequency spectrum of vibration signals. Ghalamchi and Mueller [4]

showed that the failure of multicopter propellers and motors can be detected by analyzing the vibration spectrum. Santos *et al.* [5] studied fault diagnosis techniques for wind power systems and demonstrated that SVM-based models can identify common faults, such as misalignment and imbalance. In addition, Liu *et al.* [6] summarized AI-based diagnosis methods for various rotating machines. These methods include the use of time waveforms, frequency spectra [1], [3], [4] and artificial intelligence [2], [5], [6]. However, all of these methods measure vibration data on the basis of the sampling theorem. Thus, high-speed sampling is necessary, and a large amount of data must be transferred and stored. This requires expensive measurement equipment.

In recent years, a method that uses compressed sensing (CS) has been proposed to solve this problem. CS is an alternative to the sampling theorem, and it can accurately recover images and signals using a considerably lower amount of measurement data than that typically required, provided that the measurement data are sparse to a certain basis that is incoherent. CS has been applied to fault diagnosis and monitoring and has been successfully used for data

The associate editor coordinating the review of this manuscript and approving it for publication was Li He .

compression. Bao *et al.* [7] applied CS using the Fourier basis and wavelet basis to monitor the condition of a bridge using vibration signals and showed that the signal compression ratio was higher when the wavelet basis was used. This showed that the data required for monitoring could be compressed by using CS, but not significantly because the acceleration signal was not very sparse. Zhang *et al.* [8] showed that in the diagnosis of bearing faults from vibration signals, the amount of measurement data could be significantly reduced by applying sparse coding (a type of CS), in which the basis was obtained via dictionary learning. Dang *et al.* [9] compressed the amount of data required for monitoring to 1/8 while maintaining an error of 0.06 % using dictionary learning. Therefore, as described above, the data compression ratio can be increased by using dictionary learning, and the data storage cost can be reduced. However, these methods require a high-speed logger because the data must be measured at high speed and then randomly thinned out. In contrast to these studies that apply CS to data compression, some studies have made attempts to reduce the sampling rate. Connor *et al.* [10] reduced the amount of data required for monitoring by implementing random sampling in the hardware (Narada wireless sensor) developed at the University of Michigan specifically for structural monitoring. However, this method requires dedicated hardware capable of random sampling, which increases the development cost. In this study, we developed a method for measuring data at a constant frequency with a random measurement start time (random start uniform sampling method, RSUSM) and combined it with CS. Although the performance of this method may deteriorate due to the coherence in the observation matrix, the measurement cost can be reduced because RSUSM can be realized with existing low-speed loggers. We measured the sound pressure for a failed propeller and evaluated the signal compression ratio and diagnostic accuracy of fault diagnosis using the RSUSM and CS.

The rest of the paper is organized as follows. Section 2 introduces the existing theory of compressive sensing. Section 3 describes the random sampling method implemented in this study and the newly developed RSUSM. In Section 4, the evaluation of the performance of the combination of RSUSM and CS by numerical experiments is presented. Section 5 presents the results of the application of the proposed method to diagnose a failed propeller. Finally, in section 6, a summary of this study is presented.

II. COMPRESSED SENSING

Compressed sensing is a method of estimating unknown vectors on the basis of linear observations. A measurement vector, $y \in R^m$, is obtained by the linear projection of a discrete-time signal, $s \in R^n$ ($n > m$).

$$y = \Phi s \tag{1}$$

If we represent s by an $n \times n$ orthogonal basis matrix, Ψ , with basis vectors $\{\psi_i\}$ as columns, the problem becomes

$$y = \Phi \Psi x = Ax \tag{2}$$

where $A = \Phi \Psi$ is an $m \times n$ matrix referred to as the sensing matrix, and x is the coefficient of Ψ , which is used as an unknown variable in CS. Typical orthogonal bases include the wavelet basis [11], discrete Fourier basis, and curvelet basis [12].

Dictionary learning can be used to simultaneously obtain the basis and coefficients [13]–[15]. As Eq. (2) is an under-determined linear equation, the solution is not determined. However, it has been proven that x can be accurately reconstructed under the following conditions [16], [17]:

- x is s -sparse, where a vector is defined to be s -sparse if it has at most s nonzero entries
- sensing matrix A has the restricted isometry property (RIP)

The RIP is restricted to sparse vectors. Matrix A is said to have the RIP if, for any x with s nonzero components, there exists a constant $\delta \in (0, 1)$ that satisfies

$$1 - \delta \leq \frac{x^T (A^T A) x}{x^T x} \leq 1 + \delta \tag{3}$$

The minimum value of δ , i.e., δ_s , is referred to as the RIP constant of the s^{th} order. The smaller this constant, the better the reconstruction. The l_0 -norm minimization given by

$$\hat{x} = \arg \min \|x\|_0 \quad \text{subject to } y = Ax \tag{4}$$

can be used to find the sparsest solution of Eq. (2) when $\delta_{2s} < 1$ [18]. However, as this is a combinatorial optimization problem, the required computational complexity is $O(\binom{n}{s})$, which is quite large and difficult to solve. Therefore, to obtain a relatively sparse solution, we consider a method of minimizing the l_1 norm as follows:

$$\hat{x} = \arg \min \|x\|_1 \quad \text{subject to } y = Ax \tag{5}$$

In this case, it is known that the reconstruction is successful if the condition $\delta_{2s} < \sqrt{2} - 1$ is satisfied. As this problem can be solved using linear programming, it can be solved with a computational complexity of $O(n^3)$. We consider the conditions under which the restoration succeeds for such a computer-operable l_1 minimization. When Ψ has a Wavelet or Fourier basis, Candes [19], Candes and Tao [17], and Baraniuk [20] have shown that if a Gaussian or Bernoulli random matrix is used for Φ , then A has the RIP under the following condition:

$$m > cs \log(n/s) \tag{6}$$

where c is a specific constant [21]. In addition, Candes *et al.* have shown that Φ can be constructed by randomly selecting m rows from an $n \times n$ orthogonal matrix [19]. As a specific value of c , Donoho *et al.* have shown that reconstruction is successful at $c = 2$ when A is a random matrix [22]. However, if the measurements contain noise or A is not a completely random matrix, a larger value of m may be required. In this work, we determine the values of m and the error for which reconstruction is possible.

It is well known that even if compressed measurements contain noise, sparse solutions can be obtained by solving the l_1 regularization using LASSO, as shown below [23].

$$\hat{\mathbf{x}} = \arg \min \left(\frac{1}{2} \|\mathbf{y} - \mathbf{A}\mathbf{x}\|_2^2 + \lambda \|\mathbf{x}\|_1 \right) \quad (7)$$

where λ is a nonnegative regularization parameter. The solution becomes sparser as λ increases. In this study, λ was determined by cross-validation. In the cross-validation, the mean squared error (MSE) was obtained by dividing the data into ten parts, and the largest λ within one standard error of the difference from the minimum MSE was adopted. If the solution of Eq. (7) is \mathbf{x}^* , then the error is

$$\|\mathbf{x}^* - \mathbf{x}\|_2 \leq C_0 \|\mathbf{x}^* - \mathbf{x}_s\|_1 / \sqrt{s} \quad (8)$$

$$\|\mathbf{x}^* - \mathbf{x}\|_1 \leq C_0 \|\mathbf{x}^* - \mathbf{x}_s\|_1 \quad (9)$$

where \mathbf{x}_s is a vector with s elements in the increasing order of \mathbf{x} , where s elements are unchanged and the rest are set as 0 [18]. The following equation provides constant C_0 :

$$C_0 = 2 \frac{1 + (\sqrt{2} - 1) \delta_{2s}}{1 - (\sqrt{2} + 1) \delta_{2s}} \quad (10)$$

This theorem shows that even when \mathbf{x} is not s -sparse, the restoration error can be suppressed by a constant multiple of residuals, indicating the robustness of the l_1 restoration. However, as it is difficult to directly calculate δ_{2s} , it is necessary to test and determine the error for various problems.

III. COMPRESSED SENSING METHOD FOR FAULT DIAGNOSIS

A. EXPERIMENTAL SETUP

The proposed fault diagnosis method with CS was verified using the experimental setup shown in Fig. 1. This apparatus was an open-loop system, in which room temperature (25 °C) air was blown by a propeller and discharged into the atmosphere by an exhaust pipe. A microphone installed at the pipe outlet was used to measure the change in the fluid noise caused by propeller failure. The measurements were obtained using a data logger, and the sampling rate was set as $f_s = 1000$ Hz. The measurement time was 300 s; thus, the number of measurement data points was $n = 300000$.

Fig. 2 shows the propeller used in the test. A fault was generated by changing the fin chipping length of one of the seven blades to 0, 8, 12, or 16 mm. The rotational frequency was set as $f_p \approx 64$ Hz, and thus, the blade passing frequency was $f_{pp} = f_p \times 7 \approx 450$ Hz. As both frequencies were smaller than the Nyquist frequency ($f_s/2 = 500$ Hz), it was possible to evaluate the effect of the failure using the frequency spectrum.

B. COMPRESSED SENSING BY RANDOM SAMPLING

Random sampling was realized by constructing Φ_r by randomly thinning out the original signal, \mathbf{s} . Then, \mathbf{s} was restored by identifying the Fourier coefficients, \mathbf{x}_r , using LASSO and performing reconstruction, as shown in the flow in Fig. 3(b).

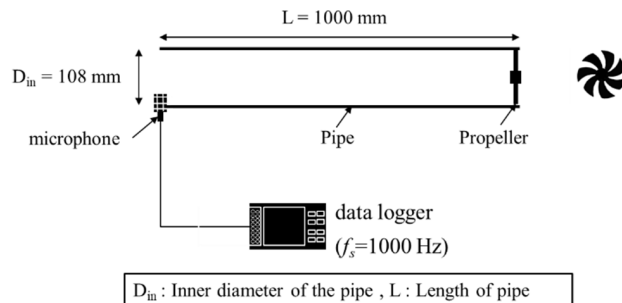


FIGURE 1. Experimental setup.



FIGURE 2. Normal propeller (left) and a failed propeller (right).

The reconstruction error, r_r , was evaluated using the following equation:

$$r_r = \|\mathbf{x} - \mathbf{x}_r\|_2^2 / \|\mathbf{x}\|_2^2 \times 100\% \quad (11)$$

The performance of data compression was evaluated on the basis of signal compression ratio α .

$$\alpha = m/n \quad (12)$$

C. COMPRESSED SENSING BY RSUSM

The RSUSM was applied by repeating the measurement of original signal \mathbf{s} at a constant frequency (f_{rsu}). Coherence was reduced by randomly executing the measurement start timing. Φ_{rsu} is given by

$$\Phi_{rsu} = [\Phi_{ij}]_n \quad (13)$$

$$\Phi_{ij} = \begin{cases} 1 & \text{if } i = j \text{ and } i = \frac{f_s}{f_{rsu}}p + \frac{f_s}{f_{rsu}}M_pq + \sum_{k=1}^q \beta_k \\ (\beta_k = \text{rand}[1, 200]) & (p = 0, 1 \dots M_p), (q = 0, 1 \dots M_q), \\ 0 & \text{otherwise} \end{cases} \quad (14)$$

where M_q is the number of times the random measurement is performed, β is a function that randomly takes values from 1 to 200, M_p indicates the number of data points in one fixed frequency measurement, f_{rsu} is a sampling frequency. f_{rsu} does not affect the performance of CS. However, deviations from the original data occur if the measurement points are unevenly distributed. Thus, we used $f_{rsu} = M_p M_q N / (N - 10 M_q)$ settings to cover the entire measurement section without deviation. M_p and M_q were also operated by defining the ratios γ in the following equation:

$$\gamma = M_p / M_q \quad (15)$$

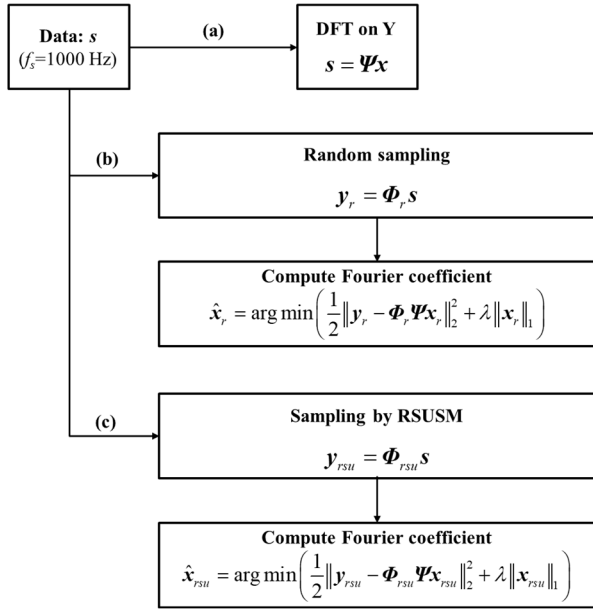


FIGURE 3. Schematic of compressed sensing with random sampling and RSUSM.

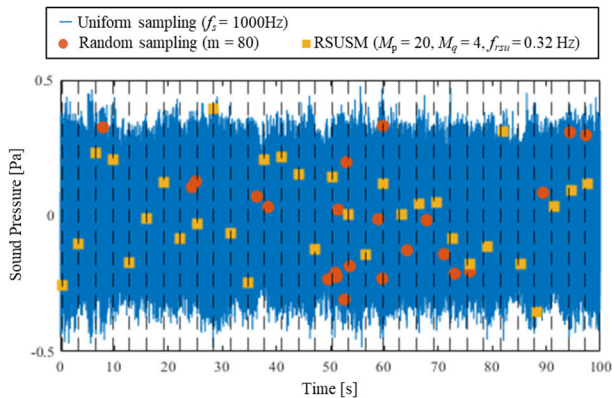


FIGURE 4. Comparison of sampling methods.

A comparison of each sampling method is shown in Fig. 4. The vertical dotted lines are drawn in 0.32 Hz increments from the first starting point of the RSUSM. Random sampling showed that the measurement was performed randomly. The RSUSM plot showed that the sampling frequency was constant for the first 20 points, but the measurement at the 21th point started randomly. In the RSUSM, this randomness made sensing matrix A close to incoherent, and thus, CS was achieved.

After the measurement, the Fourier coefficients, x_{rsu} , were identified using LASSO (Fig. 3 (c)) in the same manner as random sampling, and s was reconstructed. In this case, the reconstruction error, r_{rsu} , was set according to the following equation:

$$r_{rsu} = \frac{\|x - x_{rsu}\|_2^2}{\|x\|_2^2} \times 100\% \quad (16)$$

IV. NUMERICAL EXPERIMENT RESULTS

As the RSUSM developed in this study is a random start rather than a random sampling, A has constant coherency.

Therefore, we cannot use $c = 2$ in Eq. (6). Therefore, we conducted a new numerical experiment to find the specific constant in this method. A reconstruction experiment using CS with random sampling was conducted for the one-dimensional signal shown in the equation below. The results are shown in Fig. 5.

$$s = \sum_{f_i=1}^s D \sin(2\pi f_i t) \quad (17)$$

where $n = 1000$ and amplitude D is a random value that can take values from 1~8. CS was performed by applying Eq. (5) with a Fourier basis for Ψ . In the regions where $s < 10$ and $m < 10$, the reconstruction experiments were conducted in increments of 1. In the other regions, experiments were conducted with s and m increments of 10 and 50, respectively. The graph shows that the boundary between the successful and unsuccessful restoration regions is clearly separated, as in the results of Donoho et al [22], and this can be delimited by setting $c = 2$ in Eq. (6). In contrast, Fig. 6 shows the results of CS after sampling by RSUSM with $\gamma = 1$ using Eq. (14). From the figure, it can be seen that the performance is significantly lower than that of the boundary with $c = 2$. This is thought to be because A is not incoherent since it is sampled at a constant frequency. For the boundary between the successful and unsuccessful restoration regions, c in Eq. (6) was calculated by the least-squares method ($c = 9.84$). Fig. 7 shows the results of the numerical experiments using the same procedure with γ varying from 0.1 to 50. c is increasing logarithmically to γ . The coefficients of the logarithmic function were obtained by the least-squares method, and the following equation was found.

$$c = 1.73 \ln(\gamma) + 9.7 \quad (18)$$

When performing CS using RSUSM, operation is recommended to be within the above limitations. In actual problems, when c is too large, α exceeds 1, and CS often does not work. Therefore, we need to determine γ by considering the trade-off between the desired compression performance and the number of random sampling points. In this study, CS was conducted with $\gamma = 5$.

V. EXPERIMENTAL RESULTS

Fig. 8 shows the sound pressure waveforms in the normal and abnormal conditions. The sound pressure waveforms oscillate at high and low frequencies in the normal and abnormal conditions, respectively. Fig. 9 shows the frequency spectrum obtained using the discrete Fourier transform (DFT) for the sound pressure waveforms. There is a peak only at the blade passing frequency ($f_{pp} \approx 450$ Hz) in the normal condition and at the rotational frequency ($f_p \approx 64$ Hz) and its harmonics in the abnormal condition. This may be because the lack of a propeller causes the flow driven by the propeller to weaken once per revolution.

Thus, the changes in the rotational frequency component ($f_p \approx 64$ Hz) can be used to diagnose a failure.

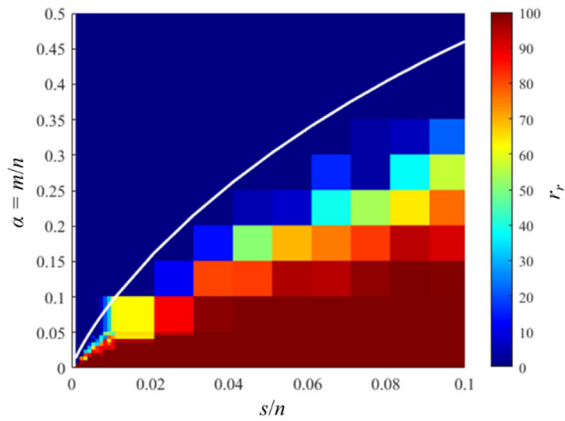


FIGURE 5. Recovery experiment by Random sampling. (The white line represents Eq.(6) at $c = 2$.)

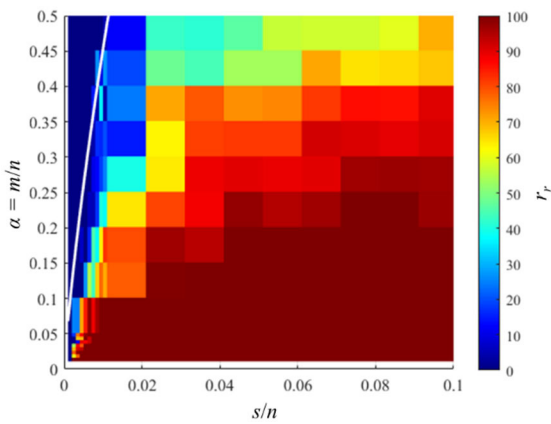


FIGURE 6. Recovery experiment by RSUSM. ($\gamma = 1$, the white line represents Eq.(6) at $c = 9.84$.)

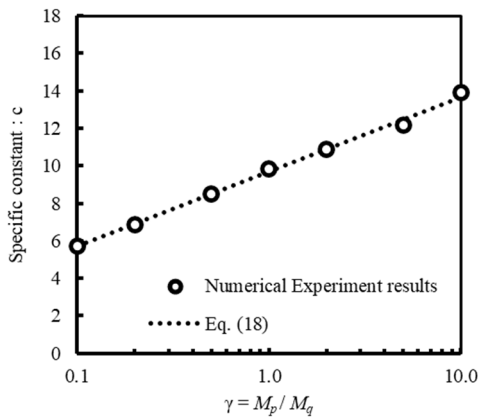


FIGURE 7. Relationship between γ and c in recovery experiments using RSUSM.

However, a measurement frequency of 128 Hz or higher is required to detect these changes. In addition, if the rotational frequency is unknown, it must be determined from the relationship between the rotational frequency and blade passing frequency, which requires a measurement frequency

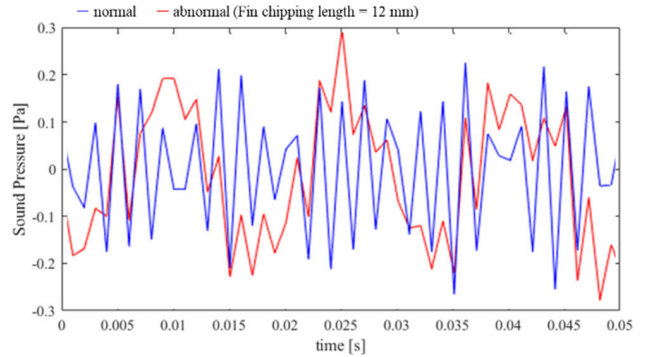


FIGURE 8. Measured sound pressure waveforms ($f_s = 1000$ Hz).

of 900 Hz or higher. Therefore, expensive measurement equipment and a large amount of data storage are required. In this study, we used CS to solve this problem. Fig. 9 shows that the Fourier coefficients become sparse when the Fourier basis is used. In the Fourier coefficients of the failure data, the amplitude of noise (components other than the rotational frequency and harmonics) is less than 0.005. Moreover, the number of components that are larger than 0.005 is $s = 27$. Assuming that all other components can be regarded as zero, Eq.(6) shows that the reconstruction is successful if there are more than $m = 504$ ($\approx 18.7s$) measurement points. However, in reality, the amplitudes of the other 27 points are not zero. In addition, the RSUSM does not entirely follow Eq. (6) because sensing observation matrix A is not incoherent. Therefore, in this study, CS was performed for $m \approx 0.2 s - 460 s$, and its performance was evaluated.

Figs. 10(a) and 10(b) show the spectrum obtained by applying CS to the data obtained using random sampling and the RSUSM with $m = 3125$ ($\approx 116 s$), respectively. The dotted lines in the figure represent the frequencies of 1st and 7th orders of rotation. Random sampling and the RSUSM can reconstruct the peaks of the rotational frequency and blade passing frequency. Random sampling reconstructs the blade passing frequency and rotational frequency amplitude more accurately compared to the RSUSM. In addition, there are fewer false estimates of peaks, and the overall error is small. This is because observation matrix A is incoherent in random sampling.

Next, to evaluate the influence of the measurement parameters on the RSUSM, sampling and CS were conducted by changing M_p , M_q , and f_{rsu} (measurement frequency). Table 1 shows the parameters used in RSUSM. We used $f_{rsu} = M_p M_q / 250$ settings to cover the entire measurement section without deviation. In actual equipment, the data volume and measurement frequency decrease with f_{rsu} . However, when f_{rsu} is small, stable operation for a long time is required to increase the number of measurement points. Therefore, the trade-off between these two aspects must be determined.

Fig. 11 shows the relationship between the number of measurement points and reconstruction error for random

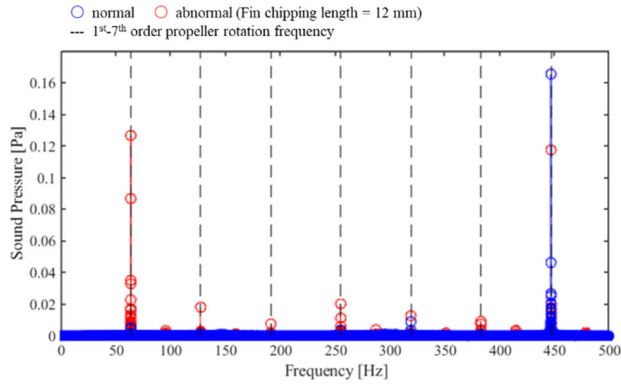


FIGURE 9. Frequency spectrum of sound pressure.

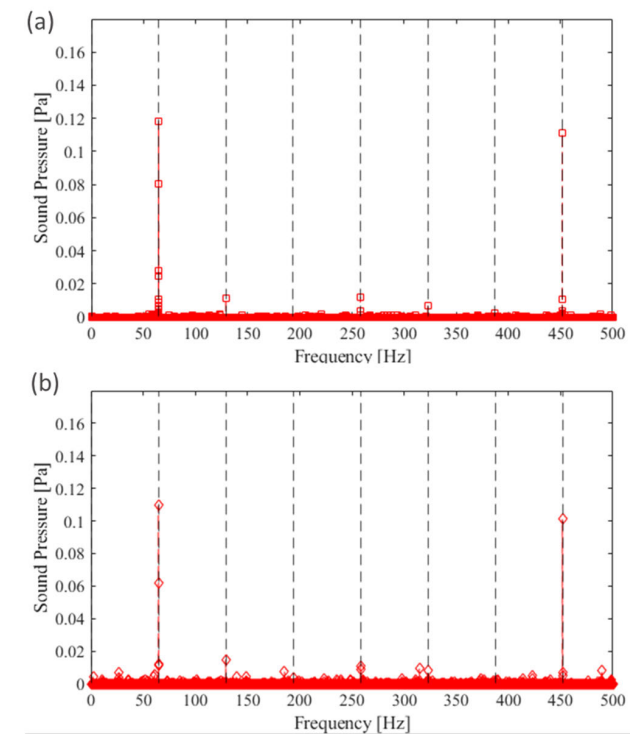


FIGURE 10. CS result of sound pressure data for a fin chipping length of 12 mm: (a) Random sampling ($m \approx 3125$), (b) RSUSM ($M_p = 125$, $M_q = 25$, $f_{rsu} = 12.5$ Hz).

sampling and the RSUSM. In the case of random sampling, the error is almost 100 % at $m = 5-80$, and it decreases rapidly as m increases to 500. However, the error does not decrease to zero even when m exceeds 504; this satisfies Eq.(6) at $c = 2$. This may be because the measurement data is not exactly s -sparse ($s = 27$) owing to noise. Therefore, to reduce m as much as possible while allowing for a certain error, it is recommended that m should be slightly larger than 504 rather than an extremely large value.

In the case of RSUSM, the error is 100 % at $m = 5-125$, and it decreases rapidly as m increases to 2000. However, the error does not decrease to zero even when m exceeds 2475; this satisfies Eq.(6) at $c = 9.84$. The reason for this may be

TABLE 1. Parameter settings in RSUSM.

M_q	M_p	f_{rsu} [Hz]	m
1	5	0.02	5
2	10	0.08	20
4	20	0.32	80
5	25	0.5	125
10	50	2	500
20	100	8	2000
25	125	12.5	3125
50	250	50	12500

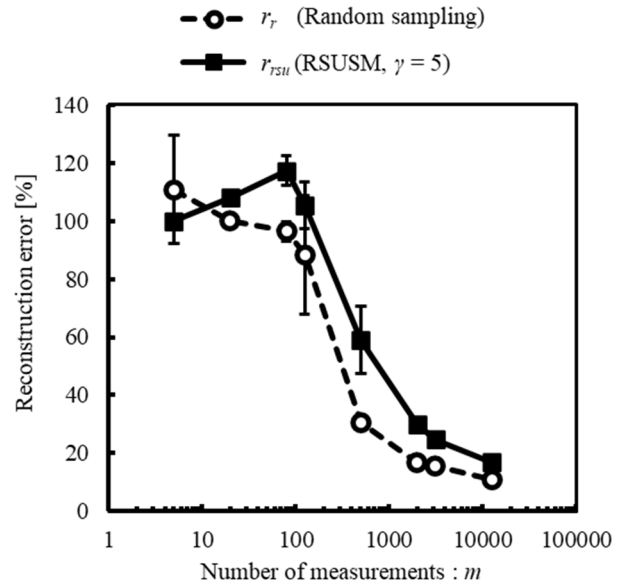


FIGURE 11. Relationship between reconstruction error and number of measurements.

the same as for random sampling. Therefore, to reduce m as much as possible while allowing for a certain error, it is recommended that m should be slightly larger than 2475 rather than an extremely large value.

At the same value of m , the error in random sampling is smaller than that in the RSUSM. However, at the almost same number of random samplings, the error in random sampling is 100 % for $m = 80$, whereas it is 17 % for the RSUSM when $M_q = 50$. Hence, the performance of the RSUSM is better. Therefore, the RSUSM is suitable when the number of random samplings cannot be increased.

Finally, to evaluate the possibility of fault diagnosis using CS, random sampling and the RSUSM with CS were applied to the data obtained for different fin chipping lengths. The trends of the rotational frequency components are plotted in Fig. 12 for each method. The results of the DFT show that the rotational frequency component increases with the propeller chipping length; this trend is also observed for random sampling and the RSUSM with CS. However, both methods

TABLE 2. Performance evaluation of CS.

	Original data	CS by RSUSM ($M_q = 25$, $M_p = 125$, $f_{rsu} = 12.5$ Hz)	CS by random sampling ($m = 3125$)	CS by random sampling ($m = 270$)
Number of data points	300000	3125	3125	270
Data size (bytes)	2400000	25000	25000	2160
α	-	0.010	0.010	0.0009
Amplitude detection error for f_p (%)	-	16	6	39
Number of random samplings	-	25	3125	270

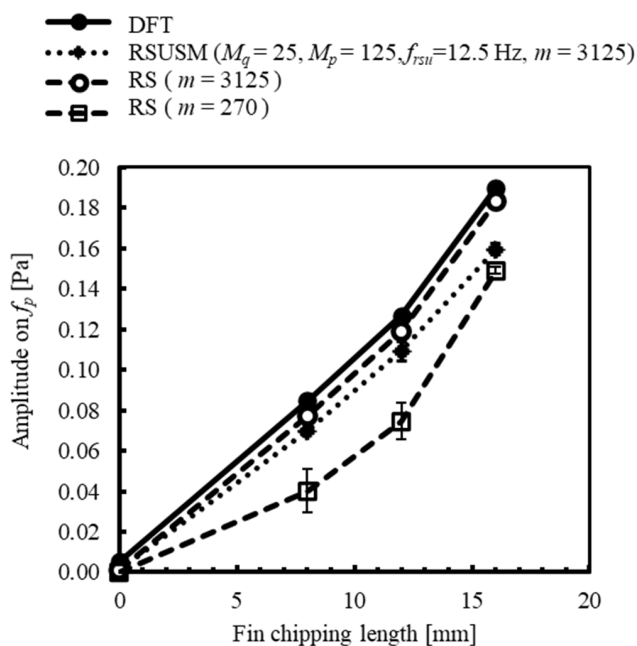


FIGURE 12. Detection results of rotational frequency components by each method.

tend to underestimate the amplitude. This is probably because the l_1 -norm is smaller when the amplitude is underestimated compared to when it is overestimated. Therefore, when CS is used for fault diagnosis, it is recommended to set the failure threshold to be smaller than the assumed error.

Table 2 shows the performance of each method in detecting the rotational frequency components using CS. For both methods, the amount of measured data is 1 % at $m = 3125$, which is significantly low. The detection error for the rotational frequency component increases m decreases from 3125 to 270. Therefore, it is necessary to consider the trade-off between data reduction and the error to determine the signal compression ratio in actual equipment. For the same number of measurement points, the performance of random sampling is better than that of the RSUSM.

However, the performance of the RSUSM with 25 random sampling points is better than that of random sampling with 270 points. Therefore, the RSUSM is suitable when random sampling points cannot be increased. The RSUSM can detect fault signals with a measurement frequency of approximately 12.5 Hz, which is 1/80 of the original data measurement frequency (1000 Hz).

M_q must be increased to further improve the performance of the RSUSM. However, the number of random samplings must be increased to increase M_q ; this requires a long measurement time. The measurement time can be decreased by increasing f_{rsu} . However, a data logger with a high measurement frequency is required, which increases the cost. Therefore, it is necessary to consider the trade-off between M_q and f_{rsu} when setting their values.

VI. CONCLUSION

To reduce the cost of measurement and data storage in fault diagnosis, a sampling method called RSUSM was developed and combined with CS. Numerical experiments demonstrated how the specific constant varies with respect to γ , which is defined as the ratio of the number of random sampling points M_q to the number of sampling points M_p at a fixed interval (Eq. (18)). This allowed us to understand the limit of how many measurement points are required for the number of non-zero components. This CS by RSUSM was validated using the sound pressure measurement data of the failed propeller. As a result, it was found that the signal could be recovered within the aforementioned limit less than 25% error even in a real environment with noise. In this case, the measurement frequency was found to be reduced to 1/80 of the frequency required by the sampling theorem. This made it possible to realize CS with an inexpensive data logger by using RSUSM. It was also found that the measurement data size could be compressed to 1%. This made it possible to reduce the data storage cost. As a result of applying the CS by RSUSM to the experimental results with different blade chipping lengths, the rotational frequency component, which is a diagnostic indicator, was identified with an average error of 16%. These results indicate that fault diagnosis can be realized with a small error and low data storage and measurement costs. Recommendations for applying CS by RSUSM for fault diagnosis include setting the threshold value low because it tends to underestimate the amplitude, and setting the values of M_q and f_{rsu} considering the trade-off between the required compression performance and measurement time. Furthermore, this method cannot be applied to signals that are non-sparse with respect to the Fourier basis because of noise or rotational speed fluctuations.

As described above, we developed a new sampling method, RSUSM, which is feasible with existing low speed loggers, and showed its performance limits by numerical experiments. The method was validated using an experimental setup with a failed propeller, and recommendations were provided for applying the method to fault diagnosis. The RSUSM is an innovative method for fault diagnosis of rotating machinery

that can simultaneously reduce the cost of measurement and data storage. This new method is expected to diagnose faults in more rotating machines.

In the future, we plan to implement the RSUSM using a microcomputer and investigate the issues by performing measurements in an actual environment. We would also like to discuss methods to reduce the number of computing cost.

ACKNOWLEDGMENT

The author thanks to the Saba from Editage Group (www.editage.com) for editing a draft of this manuscript. This research did not receive any specific grant from funding agencies in the public, commercial, or not-for-profit sectors.

REFERENCES

- [1] R. B. W. Heng and M. J. M. Nor, "Statistical analysis of sound and vibration signals for monitoring rolling element bearing condition," (in English), *Appl. Acoust.*, vol. 53, nos. 1–3, pp. 211–226, Jan./Mar. 1998, doi: [10.1016/S0003-682X\(97\)00018-2](https://doi.org/10.1016/S0003-682X(97)00018-2).
- [2] D. T. Hoang and H. J. Kang, "Rolling element bearing fault diagnosis using convolutional neural network and vibration image," *Cogn. Syst. Res.*, vol. 53, pp. 42–50, Jan. 2019, doi: [10.1016/j.cogsys.2018.03.002](https://doi.org/10.1016/j.cogsys.2018.03.002).
- [3] R. B. Randall, "A new method of modeling gear faults," *J. Mech. Design*, vol. 104, no. 2, pp. 259–267, Apr. 1982, doi: [10.1115/1.3256334](https://doi.org/10.1115/1.3256334).
- [4] B. Ghalamchi and M. Mueller, "Vibration-based propeller fault diagnosis for multicopters," in *Proc. Int. Conf. Unmanned Aircr. Syst. (ICUAS)*, 2018, pp. 1041–1047, doi: [10.1109/ICUAS.2018.8453400](https://doi.org/10.1109/ICUAS.2018.8453400).
- [5] P. Santos, L. F. Villa, A. Reñones, A. Bustillo, and J. Maudes, "An SVM-based solution for fault detection in wind turbines," *Sensors*, vol. 15, no. 3, pp. 5627–5648, Mar. 2015, doi: [10.3390/s150305627](https://doi.org/10.3390/s150305627).
- [6] R. Liu, B. Yang, E. Zio, and X. Chen, "Artificial intelligence for fault diagnosis of rotating machinery: A review," *Mech. Syst. Signal Process.*, vol. 108, pp. 33–47, Aug. 2018, doi: [10.1016/j.ymssp.2018.02.016](https://doi.org/10.1016/j.ymssp.2018.02.016).
- [7] Y. Bao, J. L. Beck, and H. Li, "Compressive sampling for accelerometer signals in structural health monitoring," *Struct. Health Monit.*, vol. 10, no. 3, pp. 235–246, May 2011, doi: [10.1177/14759217110373287](https://doi.org/10.1177/14759217110373287).
- [8] X. Zhang, N. Hu, L. Hu, L. Chen, and Z. Cheng, "A bearing fault diagnosis method based on the low-dimensional compressed vibration signal," *Adv. Mech. Eng.*, vol. 7, no. 7, Jul. 2015, Art. no. 168781401559344, doi: [10.1177/1687814015593442](https://doi.org/10.1177/1687814015593442).
- [9] X. J. Dang, F. H. Wang, and D. X. Zhou, "Compressive sensing of vibration signals of power transformer," in *Proc. IEEE Int. Conf. High Voltage Eng. Appl. (ICHVE)*, Beijing, China, Sep. 2020, pp. 1–4.
- [10] S. M. O'Connor, J. P. Lynch, and A. C. Gilbert, "Compressed sensing embedded in an operational wireless sensor network to achieve energy efficiency in long-term monitoring applications," *Smart Mater. Struct.*, vol. 23, no. 8, Jul. 2014, Art. no. 085014, doi: [10.1088/0964-1726/23/8/085014](https://doi.org/10.1088/0964-1726/23/8/085014).
- [11] S. Mallat, *A Wavelet Tour of Signal Processing*. New York, NY, USA: Academic, 1999.
- [12] E. Candes and D. L. Donoho, "Curvelets: A surprisingly effective non-adaptive representation of objects with edges," *Curves Surf. Fitting*, vol. C., no. 2, pp. 1–10, Apr. 2000.
- [13] M. Aharon, M. Elad, and A. Bruckstein, "K-SVD: An algorithm for designing overcomplete dictionaries for sparse representation," *IEEE Trans. Signal Process.*, vol. 54, no. 11, pp. 4311–4322, Nov. 2006, doi: [10.1109/TSP.2006.881199](https://doi.org/10.1109/TSP.2006.881199).
- [14] H. Rauhut, K. Schnass, and P. Vandergheynst, "Compressed sensing and redundant dictionaries," *IEEE Trans. Inf. Theory*, vol. 54, no. 5, pp. 2210–2219, May 2008, doi: [10.1109/TIT.2008.920190](https://doi.org/10.1109/TIT.2008.920190).
- [15] E. J. Candès, Y. C. Eldar, D. Needell, and P. Randall, "Compressed sensing with coherent and redundant dictionaries," *Appl. Comput. Harmon. Anal.*, vol. 31, no. 1, pp. 59–73, Jul. 2011, doi: [10.1016/j.acha.2010.10.002](https://doi.org/10.1016/j.acha.2010.10.002).
- [16] E. J. Candès and T. Tao, "Decoding by linear programming," *IEEE Trans. Inf. Theory*, vol. 51, no. 12, pp. 4203–4215, Dec. 2005, doi: [10.1109/TIT.2005.858979](https://doi.org/10.1109/TIT.2005.858979).
- [17] E. J. Candès and T. Tao, "Near-optimal signal recovery from random projections: Universal encoding strategies?" *IEEE Trans. Inf. Theory*, vol. 52, no. 12, pp. 5406–5425, Dec. 2006, doi: [10.1109/TIT.2006.885507](https://doi.org/10.1109/TIT.2006.885507).
- [18] E. J. Candès, "The restricted isometry property and its implications for compressed sensing," *Comp. Rendus Math.*, vol. 346, nos. 9–10, pp. 589–592, May 2008, doi: [10.1016/j.crma.2008.03.014](https://doi.org/10.1016/j.crma.2008.03.014).
- [19] E. J. Candès, "Compressive sampling," *Proc. Int. Congr. Math. Madrid, Spain*, vol. 2006, pp. 22–30, Aug. 2006.
- [20] R. G. Baraniuk, "Compressive sensing [lecture notes]," *IEEE Signal Process. Mag.*, vol. 24, no. 4, pp. 118–121, Jul. 2007, doi: [10.1109/MSP.2007.4286571](https://doi.org/10.1109/MSP.2007.4286571).
- [21] E. J. Candès, J. Romberg, and T. Tao, "Robust uncertainty principles: Exact signal reconstruction from highly incomplete frequency information," *IEEE Trans. Inf. Theory*, vol. 52, no. 2, pp. 489–509, Feb. 2006, doi: [10.1109/TIT.2005.862083](https://doi.org/10.1109/TIT.2005.862083).
- [22] D. L. Donoho and J. Tanner, "Exponential bounds implying construction of compressed sensing matrices, error-correcting codes, and neighborly polytopes by random sampling," *IEEE Trans. Inf. Theory*, vol. 56, no. 4, pp. 2002–2016, Apr. 2010, doi: [10.1109/TIT.2010.2040892](https://doi.org/10.1109/TIT.2010.2040892).
- [23] R. Tibshirani, "Regression shrinkage and selection via the lasso," *J. Roy. Statist. Soc., B Methodol.*, vol. 58, no. 1, pp. 267–288, 1996, doi: [10.1111/j.2517-6161.1996.tb02080.x](https://doi.org/10.1111/j.2517-6161.1996.tb02080.x).



YUKI KATO received the M.E. degree in fluid dynamics from Tsukuba University, Tsukuba, Japan, in 2016. He is currently an Assistant Professor with the National Institute of Technology, Hiroshima College. His research interests include the fault diagnosis of rotational machines, heat transfer analysis for pulsating flow, and imaging of oscillation phenomena.

• • •